Towards artificial photosynthesis on the lipid bilayer of liposomes

Klein, D.M.

Chapter 4

A stable alkylated cobalt catalyst for photocatalytic H_2 generation in liposomes

*Photocatalytic proton reduction is a promising way to produce dihydrogen (H_2) in a clean and sustainable manner, and mimicking nature by immobilising proton reduction catalysts and photosensitisers on liposomes is an attractive approach for biomimetic solar fuel production in aqueous solvents. Current photocatalytic proton reduction systems on liposomes are, however, limited by the stability of the catalyst. To overcome this problem, we synthesised a new alkylated cobalt(II) polypyridyl complex (**CoC_{12}**), immobilised it on the lipid bilayer of liposomes, and studied its performance in a photocatalytic system containing an alkylated ruthenium photosensitiser (**RuC_{12}**) and a 1:1 mixture of sodium ascorbate and tris-2-carboxyethylphosphine hydrochloride as sacrificial electron donors. Several parameters (concentration of **CoC_{12}** and **RuC_{12}**, pH, membrane composition) were changed to optimise the turnover number for H_2 production. Overall, **CoC_{12}** was found to be photostable and the optimised turnover number (161) was limited only by the decomposition of the ruthenium-based photosensitiser.*

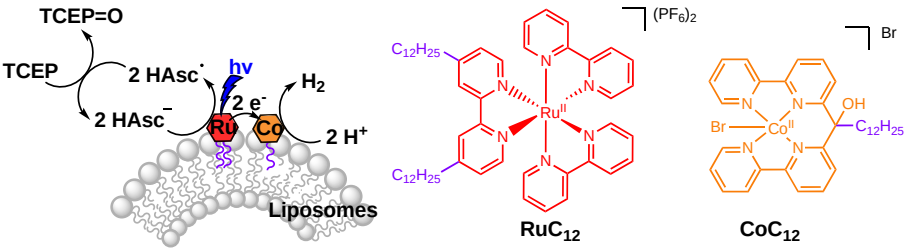

This chapter has been accepted as a full paper: David M. Klein, Leonardo Passerini, Martina Huber and Sylvestre Bonnet, *ChemCatChem* **2022**, *accepted*.

4.1. Introduction

Photocatalytic water splitting into dioxygen (O_2) and dihydrogen (H_2) is a promising approach to store sunlight in chemical bonds (H_2), and hence a potential green solution to solve the current energy crisis.[1] Photocatalytic water splitting consists of two half-reactions, i.e. water oxidation and proton reduction. A common way to investigate these half reactions is by studying three-component systems containing a catalyst (i.e. a water oxidation catalyst or a proton reduction catalyst), a photosensitiser, and an electron acceptor (for water oxidation) or an electron donor (for proton reduction).[2] In nature, such light-driven half-reactions occur in the presence of a lipid membrane, i.e., the thylakoid membrane in plants, which enables precise spatial organisation of the catalysts, light-harvesting molecules, and electron transporters. Overall, compartmentalisation of the different half-reactions in or around lipid membranes minimises charge recombination and other undesired side reactions.[3] Mimicking nature with artificially constructed lipid-based photocatalytic liposomes is therefore an appealing strategy for biomimetic solar fuel production.[3–5] Liposomes are spherical supramolecular assemblies of lipids that define two aqueous phases, i.e. an inner compartment and the exterior bulk aqueous phase, and one hydrophobic phase, i.e., the interior of the lipid bilayer. As a consequence, liposomes can be exploited for solubilising both polar as well as nonpolar molecules in an aqueous solution. With liposomes, catalysts and photosensitisers, which are only soluble in purely organic solvents or in a mixture of water and organic solvents,[6–9] can also be studied in aqueous conditions.

Up to now, the number of published liposome systems that are capable of performing photocatalytic half-reactions, such as water oxidation[10,11], proton reduction[12–15], or carbon dioxide reduction[16–18], is limited. For liposome-based proton reduction, the two only catalysts studied so far, i.e., an amphiphilic cobaloxime complex and an [Fe-Fe] hydrogenase mimic, decomposed during photocatalysis, which limited the photoreaction.[12,13,15] To restore photocatalytic activity, it was either required to add free ligand in the case of the cobaloxime complex, or to add more catalyst in the case of

the [Fe-Fe] hydrogenase mimic.[12,13,15] Therefore, a more stable catalyst is required that would allow for running photocatalytic proton reduction on liposomes for a longer time. Co(II) polypyridyl complexes are good catalyst candidates, as they are known to be photostable, exhibit good photocatalytic performance for proton reduction in aqueous media, and because cobalt is an earth-abundant metal.[19–23]

We hence prepared the alkylated cobalt polypyridyl complex **CoC$_{12}$** (Figure 4.1), immobilised it on liposomes, and studied its photocatalytic performance in the presence of a known alkylated ruthenium-based photosensitiser (**RuC$_{12}$**)[17] in the membrane, and of a mixture of sodium ascorbate (NaHAsc) and tris-2-carboxyethylphosphine hydrochloride (TCEP) in the aqueous phase as sacrificial electron donors (Figure 4.1). In such conditions, it is usually assumed that after reductive quenching of the excited photosensitiser **RuC$_{12}$*** by HAsc$^-$, TCEP is capable of recycling the 1-electron oxidised ascorbate radical (HAsc$^\bullet$) back to HAsc$^-$, which is known to enhance photocatalytic hydrogen production.[24] We varied the concentrations of the proton reduction catalyst **CoC$_{12}$** and of the photosensitiser **RuC$_{12}$**, the pH of the solution, and the lipid composition of the liposomes, to optimise this system. Finally, we investigated whether, in optimised conditions, decomposition of the catalyst, or decomposition of the photosensitiser, limited H_2 production.

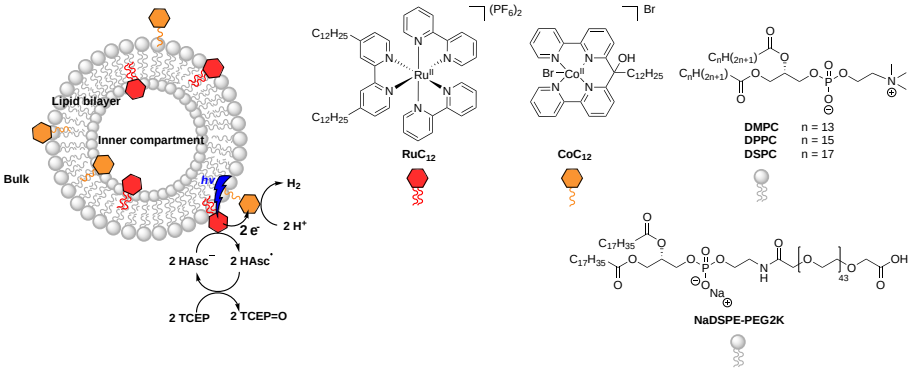

Figure 4.1. Formulae and naming of the alkyl-tail functionalised ruthenium photosensitiser (**RuC$_{12}$**, red), of the alkyl-tail functionalised cobalt catalyst (**CoC$_{12}$**, orange), and of the lipids (grey) used for photocatalytic H_2 evolution on liposomes.

4.2. Results and Discussion

4.2.1. Catalyst synthesis and preparation of photocatalytic liposomes

The amphiphilic derivative **RuC_{12}** of the well-known photosensitiser $[Ru(bpy)_3]^{2+}$ was prepared by bis-alkylation of one of the bipyridine ligands with $C_{12}H_{25}$ chains, following literature procedures.[17] The new cobalt catalyst **CoC_{12}** is based on a homogeneous catalyst developed by Alberto and co-workers.[20,24,25] It was prepared by the alkylation of the easily accessible di([2,2-bipyridin]6-yl)methanone with one $C_{12}H_{25}$ chain in a two-step process, and it was characterised by TLC, NMR, mass spectrometry, and elemental analysis, as described in the experimental part. The oxidation state of the cobalt centre was estimated using Evans' method in MeOD at 20 °C.[26] An effective magnetic moment was found to be 4.28 μ_B, which is in agreement with the presence of one high-spin Co(II) centre with three unpaired electrons.[27] Indeed, this observation was further confirmed by EPR measurements, which showed a broad EPR feature that is typical for a high spin Co(II) species (Figure D1, see Appendix D). Furthermore, the redox potentials of **CoC_{12}** in acetonitrile (Figure D2), *i.e.*, –1.24 and –1.54 V vs. Fc/Fc^+, are in agreement with that of similar complexes reported in literature.[28] Thus, the reduced **RuC_{12}^-** ($Ru^{2+/+}$ = –1.70 V vs Fc/Fc^+ in acetonitrile)[17], formed after reductive quenching of the excited photosensitiser **RuC_{12}^*** by $HAsc^-$, is thermodynamically speaking capable of reducing twice **CoC_{12}**.

Functionalised liposomes for photocatalytic H_2 evolution were prepared by mixing the two metal complexes with either 1,2-dimyristoyl-*sn*-glycero-3-phosphocholine (DMPC), 1,2-dipalmitoyl-*sn*-glycero-3-phosphocholine (DPPC), or 1,2-distearoyl-*sn*-glycero-3-phosphocholine (DSPC), in organic solvents. 1,2-distearoyl-*sn*-glycero-3-phosphoethanolamine N-(carboyl-methoxypolyethylene glycol-2000) (NaDSPE-PEG2K) was added (1 mol%) to the liposome formulation, as it is known to stabilise liposome suspensions by avoiding aggregation.[11] Thorough evaporation of the organic solvents and hydration with an aqueous solution containing an equimolar mixture of the electron donors NaHAsc (0.1 M) and TCEP (0.1 M) at pH 3, 4, 5, or 6, several

freeze-thawing cycles, and standard extrusion through a 0.2 μm polycarbonate filter, afforded photocatalytic liposomes characterised by the formula lipid:NaDSPE-PEG2K:**RuC_{12}**:**CoC_{12}** 100:1:X:Y, where lipid is DMPC, DPPC, or DSPC, X = 0.5 or 1 mol%, and Y = 0.02, 0.1, 0.5, or 1 mol%. The liposome samples were characterised by dynamic light scattering, which afforded their average diameter (Z_{ave}) and polydispersity index (PDI). Z_{ave} was typically found to be 145 – 205 nm and PDI values were below 0.20, which indicated a uniform size distribution (Table D1). As a note, bulk concentrations of 50 μM (**RuC_{12}**) and 5 μM (**CoC_{12}**) in 178 nm diameter DPPC liposomes correspond to local concentrations of 12 and 1.2 mM in the volume of the lipid bilayer, respectively (see Appendix D): due to the small ratio of the bilayer, compared to the bulk volume of the sample, supporting the photosensitiser and catalyst on the bilayers increases their concentrations by a factor ~240.

4.2.2. Photocatalytic H_2 reduction.

Photocatalytic H_2 evolution experiments were conducted by shining blue light (λ_{irr} = 450 nm, P = 10.6 mW) on the photocatalytic liposomes in argon-saturated aqueous solutions. The formation of the product H_2 in the gas phase above the irradiated solution was measured by a Clark H_2 sensor, which was integrated within an in-house assembled set-up.[29] Prior to irradiation, each liposome solution was left in the dark for 1 h, which in all cases did not result in any H_2 formation. Then, the solution was irradiated with blue light for 19 h.

The photocatalytic performances of all tested photocatalytic liposome solutions are summarised in Table 4.1. Here, TON is the turnover number (defined as TON = n_{H2}/n_{CoC12}) and PTON the photocatalytic turnover number (defined as PTON = $2 \times n_{H2}/n_{RuC12}$; the factor 2 accounts for the fact that 2 molecules of photosensitiser must turnover once for the formation of one H_2 molecule). The (photocatalytic) turnover frequency ((P)TOF) is defined as the maximum number of (P)TON per unit time at the highest rate of H_2 production. In order to optimise the photocatalytic performance of the **CoC_{12}**-**RuC_{12}** liposomal system, we varied the concentrations of **CoC_{12}** (1, 5,

25, and 50 μM) and of **RuC_{12}** (25 and 50 μM), the pH of the solution (3 – 6), and the type of lipid in the membrane (DMPC, DPPC, or DSPC), which influences its fluidity at the temperature used for photocatalysis (298 K). All other parameters (i.e. the light intensity and the concentration of the electron donors) were kept constant. Dynamic light scattering measurements were carried out to monitor changes in the size of the liposomes when running photocatalysis. In all cases except at pH = 6 (see below), the hydrodynamic radius after irradiation did not differ much (< 10 nm) compared with that before irradiation, suggesting that the photocatalytic liposomes remained essentially intact in such conditions (Table D1). Control experiments performed in absence of one of each component (Table 4.1, Figure D3) confirmed that no H_2 evolved when any one of them were absent from the catalytic mixture. Notably, no photocatalytic activity was observed in absence of TCEP, although many hydrogen evolution systems based on ruthenium-based photosensitisers and cobalt-based catalysts are reported to operate with solely $HAsc^-$ as sacrificial electron donor.[30]

As a note, as shown in Table 4.1 and Figure 4.2 the margin of error is larger with photocatalytic liposomes than that observed in homogeneous conditions. We attribute these experimental variations to the large number of steps necessary to prepare liposome samples. For example, liposome preparation includes many freeze/thawing cycles, which may take place at different rates; extrusion requires pressure, which is applied by hand. Lastly, the time between the preparation of the liposomes and the start of the photocatalytic experiment, is likely to be different for each sample. Even when no obvious signs of aggregation can be seen experimentally by DLS, it still might occur in the dark, slightly changing the photocatalytic results compared to samples which were used directly after preparation. All in all, analysing trends based on a single replicate is impossible, and reproducing at least three independent experiments is a must for studying photocatalytic liposomes.

Table 4.1. Photocatalytic H_2 generation with liposomes prepared from mixtures of a lipid (DMPC, DPPC, or DSPC), NaDSPE-PEG2K, NaHAsc, TCEP, **RuC_{12}**, and **CoC_{12}**, upon blue light irradiation.[a]

Lipid	[NaHAsc]	[TCEP]	[RuC_{12}]	[CoC_{12}]	pH	n H_2[b,c]	TON[c]	TOF[d]	PTON[c]	PTOF[d]
DPPC	0.1 M	0.1 M	50 µM	50 µM	5.0	6.8 ± 3.2	39 ± 18	8.4 ± 2.2	78 ± 36	17 ± 4
DPPC	0.1 M	0.1 M	50 µM	25 µM	5.0	7.1 ± 2.2	81 ± 25	19 ± 5	81 ± 25	19 ± 5
DPPC	0.1 M	0.1 M	50 µM	5 µM	5.0	1.9 ± 0.8	107 ± 46	25 ± 8	21 ± 9	4.9 ± 1.6
DPPC	0.1 M	0.1 M	50 µM	1 µM	5.0	0.3 ± 0.3	n.d.[e]	n.d.[e]	n.d.[e]	n.d.[e]
DPPC	0.1 M	0.1 M	50 µM	5 µM	3.0	1.6 ± 1.2	92 ± 69	43 ± 1	18 ± 14	8.5 ± 0.2
DPPC	0.1 M	0.1 M	50 µM	5 µM	4.0	2.8 ± 0.7	161 ± 41	86 ± 22	32 ± 8	17 ± 4
DPPC	0.1 M	0.1 M	50 µM	5 µM	6.0	2.6 ± 0.6	149 ± 34	16 ± 3	30 ± 7	3.1 ± 0.6
DPPC	0.1 M	0.1 M	25 µM	5 µM	5.0	1.0 ± 0.7	58 ± 43	7.0 ± 0.7	23 ± 17	2.8 ± 0.3
DMPC	0.1 M	0.1 M	50 µM	5 µM	4.0	1.2 ± 0.5	68 ± 27	74 ± 35	14 ± 5	15 ± 7
DSPC	0.1 M	0.1 M	50 µM	5 µM	4.0	1.5 ± 0.9	87 ± 51	25 ± 5	17 ± 10	5.1 ± 1.0
DPPC	0.1 M	0.1 M	50 µM	-	5.0	0.4	-	-	5	2.9
DPPC	0.1 M	0.1 M	-	25 µM	5.0	-	-	-	-	-
DPPC	0.1 M	-	50 µM	25 µM	5.0	0.4	5	1.9	5	1.9
DPPC	-	0.1 M	50 µM	25 µM	5.0	-	-	-	-	-

[a] Bulk concentrations: [lipid] = 5 mM, [NaDSPE-PEG2K] = 50 µM, t_{irr} = 19 h, λ_{irr} = 450 nm, P = 10.6 mW, photon flux (Φ_0) = 13.7 nmol/s (see Appendix D for the derivation and Figure D4). Conditions: argon-saturated solutions, volume 3.5 mL, temperature 25 °C. The values and standard deviations are derived from the average of three replicate experiments. Control experiments were performed once. [b] in µmol. [c] at t = 20 h. [d] in h^{-1}. [e] The error on the measurement was too high to determine these values, because the amount of H_2 generated was near the detection limit of the sensor.

Varying the concentration of CoC_{12} and RuC_{12}. When the amount of catalyst **CoC_{12}** in the DPPC membrane was decreased (50, 25, 5, 1 µM) at constant photosensitiser concentration (50 µM), the TON and TOF increased (Figure 4.2), from 39 ± 18 and 8.4 ± 2.2 h^{-1}, respectively, for 50 µM **CoC_{12}**, up to 107 ± 46 and 25 ± 8 h^{-1}, respectively, for 5 µM **CoC_{12}**. Unfortunately, the TON could not be determined when the concentration of **CoC_{12}** was lowered down to 1 µM, because in such conditions the amount of H_2 produced (0.3 ± 0.3 µmol) became very low, within the range of the signal noise of the H_2 detector. Still, the productivity and rate of the catalyst improved when its concentration was decreased down to 5 µM, suggesting that high concentrations of the cobalt catalyst in the membrane are detrimental to the overall photocatalytic process.

On the other hand, the PTON and PTOF both decreased when the amount of **CoC_{12}** in the DPPC membrane was lowered, from 78 ± 36 and 17 ± 4 h^{-1}, respectively, for 50 µM **CoC_{12}**, down to 21 ± 9 and 4.9 ± 1.6 h^{-1}, respectively, for 5 µM **CoC_{12}**. These results clearly indicate that the stability of the

photosensitiser is limiting the photocatalytic system. Decreasing the concentration of the photosensitiser **RuC$_{12}$** from 50 µM to 25 µM also leads to a less efficient photocatalytic system, as almost half the amount of hydrogen was produced (TON = 58 ± 43), while the maximum hydrogen production rate became 2-3 times slower (TOF = 7.0 ± 0.7 h^{-1} and PTOF = 2.8 ± 0.3 h^{-1}). The PTON remained constant within experimental errors (from 21 ± 9 to 23 ± 17), while we would have expected the same H_2 production, hence a doubled PTON, if the catalyst would decompose. Based on these data, it was decided to keep a photosensitiser concentration of 50 µM in the membrane during further optimisation. In addition, most probably the rate-determining step of the photocatalytic system as a whole, involves the photosensitiser molecule.

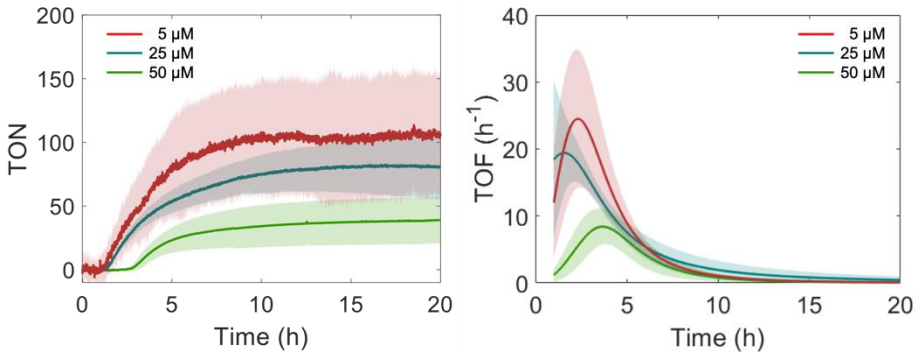

Figure 4.2. Photocatalytic activity of liposomes consisting of DPPC:NaDSPE-PEG2K:**RuC$_{12}$**:**CoC$_{12}$** with varying catalyst concentration [**CoC$_{12}$**]. The samples were left in the dark for 1 h and then irradiated with blue light for 19 h. Each curve is the average of the data of three replicates and includes the standard deviation (shaded area). Experimental conditions: [DPPC] = 5 mM, [NaDSPE-PEG2K] = 50 µM, [**RuC$_{12}$**] = 50 µM; argon-saturated 0.1 M NaHAsc and 0.1 M TCEP aqueous solution, volume 3.5 mL, temperature 25 °C, λ_{irr} = 450 nm, P = 10.6 mW, Φ_0 = 13.7 nmol/s. Bulk concentrations [**RuC$_{12}$**] and [**CoC$_{12}$**] indicate theoretical concentrations assuming no losses during liposome preparation.

Varying the pH. As the next step, we investigated whether the pH of the solution may have an effect on photocatalysis. Typically, higher proton concentrations make proton reduction catalysts faster, until catalyst decomposition or protonation of the electron donor start to take place. As a note, in all experiments the pH of the liposome solution did not change much (< 0.5) upon light irradiation for 19 h (Table D1). With this system, the highest

photocatalytic performance was obtained at pH 4.0 (Figure 4.3). In more acidic conditions (pH = 3.0), the lower concentration of the ascorbate electron donor $HAsc^-$ (pKa = 4.0, $H_2Asc \rightarrow H^+ + HAsc^-$)[2,31] is likely to negatively influence photocatalysis. In less acidic conditions (pH = 6.0), aggregation of the liposomes occurred, as observed by dynamic light scattering after photocatalysis (Table D1). It is unclear how such aggregation influences the photocatalytic mechanism, but clearly, the photocatalytic rate of the DPPC liposomes at pH 6 was lower (TOF = 16 ± 3 h^{-1} compared to TOF = 86 ± 22 h^{-1} at pH 4), while the system was still active after 19 h light irradiation, suggesting a higher stability. Overall, the photocatalytic rate was maximal at pH 4, which we hence considered as the optimal condition for this system.

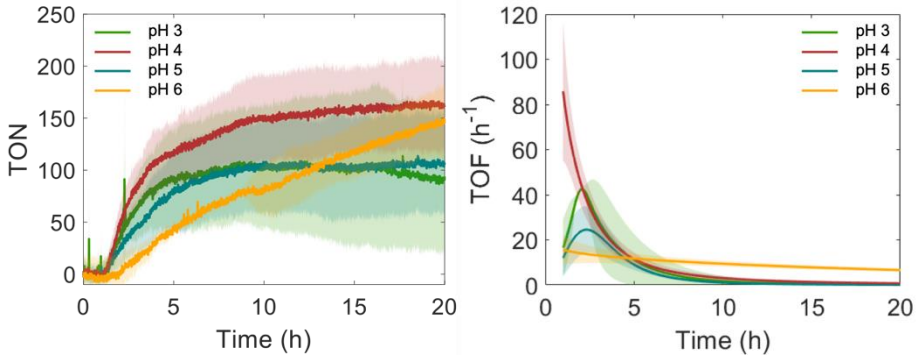

Figure 4.3. Photocatalytic activity of DPPC:NaDSPE-PEG2K:**RuC_{12}**:**CoC_{12}** 100:1:1:0.1 liposomes at varying pH. The samples were left in the dark for 1 h and then irradiated with blue light for 19 h. Each curve is the average of three replicates and includes the standard deviation (shaded area). Experimental conditions: [DPPC] = 5 mM, [NaDSPE-PEG2K] = 50 µM, [**RuC_{12}**] = 50 µM, and [**CoC_{12}**] = 5 µM; argon-saturated 0.1 M NaHAsc and 0.1 M TCEP aqueous solution, volume 3.5 mL, temperature 25 °C, λ_{irr} = 450 nm, P = 10.6 mW, Φ_0 = 13.7 nmol/s. Bulk concentrations [**RuC_{12}**] and [**CoC_{12}**] indicate theoretical concentrations assuming no losses during liposome preparation.

Varying the lipid. To investigate the influence of the phospholipid on photocatalysis, we embedded **CoC_{12}** (5 µM) and **RuC_{12}** (50 µM) in three different membranes prepared from the saturated lipids DMPC, DPPC, or DSPC. We did not include unsaturated lipids such as 1,2-dioleoyl-*sn*-glycero-3-phosphocholine (DOPC) in this study, because their membrane has been reported to be photochemically instable.[3] A membrane can exist in different phases, such as the liquid crystalline phase, which results in a more flexible

and mobile membrane, or the gel phase, a more rigid membrane. The phase transition temperature T_m, at which the membrane goes from the gel phase to the liquid crystalline phase, increases from DMPC (T_m = 23 °C) to DPPC (T_m = 41 °C) and DSPC (T_m = 55 °C). There is currently no fundamental understanding about which phase of the membrane is better for photocatalysis; in some cases photocatalysis occurs better in the gel phase, in other cases better in the liquid crystalline phase.[3] In our experiments run at 25 °C, both DPPC and DSPC membranes were in the gel phase, while DMPC was near the transition temperature. According to our data, the nature of the lipid had a dramatic effect on the TON; **CoC_{12}** and **RuC_{12}** were much more active in a DPPC membrane (TON = 161 ± 41) than in a DMPC (TON = 68 ± 27) or DSPC membrane (TON = 87 ± 51) (Figure 4.4). Thus, for this particular photocatalytic system, a rigid and stable DPPC membrane was preferred over a mobile DMPC membrane, but the membrane should not be too rigid (DSPC).

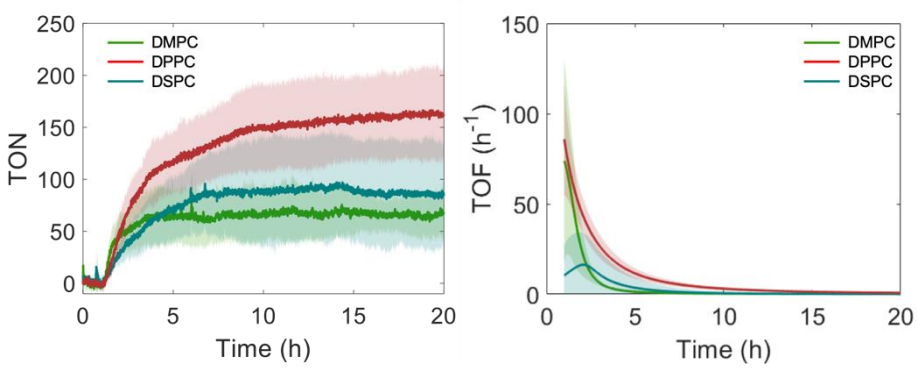

Figure 4.4. Photocatalytic activity of liposomes consisting of lipid:NaDSPE-PEG2K:**RuC_{12}**:**CoC_{12}** 100:1:1:0.1, where lipid is either DMPC, DPPC, or DSPC. The samples were left in the dark for 1 h and afterwards irradiated with a blue light for 19 h. Each curve is the average of three replicates and includes the standard deviation (shaded area). Experimental conditions: [DMPC, DPPC, or DSPC] = 5 mM, [NaDSPE-PEG2K] = 50 µM, [**RuC_{12}**] = 50 µM, and [**CoC_{12}**] = 5 µM; argon-saturated 0.1 M NaHAsc and 0.1 M TCEP aqueous solution, volume 3.5 mL, pH = 4.0, temperature 25 °C, λ_{irr} = 450 nm, P = 10.6 mW, Φ_0 = 13.7 nmol/s. Bulk concentrations [**RuC_{12}**] and [**CoC_{12}**] indicate theoretical concentrations assuming no losses during liposome preparation.

Stability of the system. As determined by the experiments described above, under fully optimised conditions (DPPC lipid, 5 µM CoC_{12}, 50 µM RuC_{12}, pH

4), the TON was equal to 161 ± 41 with a quantum yield of 2.9% after 1 h of irradiation (see Appendix D for the calculation), which is comparable to our knowledge to the highest TON reported for H_2 evolution on photocatalytic liposomes with purely molecular catalysts and photosensitisers.[12] On the other hand, with **CoC_{12}** it was not required to add excess ligand during irradiation to reach such H_2 production, which is an advantage. Still, after the first hour of light irradiation, H_2 generation slowed down and after 19 h of irradiation no significant H_2 production was observed anymore, which was a sign of decomposition of at least one of the components of the photocatalytic system. To obtain some insight into the reasons for the limitations of photocatalysis, we added either an additional equivalent of fresh photosensitiser (**RuC_{12}**), or an equivalent of fresh catalyst (**CoC_{12}**), to the reaction mixture after a first photocatalytic run. In previous work[13], such replenishment of active molecules had been made by adding freshly-prepared liposomes containing solely the photosensitiser, to the irradiated reaction mixture. In such conditions, dilution of the reaction mixture may occur, and migration of the photosensitiser molecules from the freshly added liposomes to the irradiated, catalyst-containing vesicles, was not 100% sure. To avoid these effects, here we prepared a thin film of either **RuC_{12}** or **CoC_{12}** in a glass pressure-resistant tube, added the irradiated liposome reaction mixture to this flask, and heated the solution for 1 h at 50 °C while gently vortex-mixing the solution every 15 min. By doing so, we aimed at maximising the insertion of the photosensitiser molecules, from the thin film into the irradiated liposomes. Upon resuming light irradiation, we observed that the addition of extra **RuC_{12}** prolonged the photocatalytic activity by a supplemental TON = 75, whereas the addition of extra **CoC_{12}** did not lead to any extra H_2 production (Figure 4.5A). This experiment demonstrated that the stability of **RuC_{12}** clearly limited H_2 evolution during the first photocatalytic run. UV-Vis spectroscopy further demonstrated that the characteristic ^{3}MLCT absorption band of **RuC_{12}**, observed between 410 and 470 nm, had almost completely disappeared after 19 h of irradiation of the photocatalytic liposomes (Figure 4.5B). An increase in absorption was observed between 500 and 700 nm that is typical for a $[Ru(bpy)_2(H_2O)_2]^{2+}$ decomposition product.[32] Such a species is probably formed after photolabilisation of either a bpy-C_{12} ligand or a bpy ligand, which was

reported as a decomposition pathway in acidic aqueous conditions.[16,33] Overall these experiments demonstrated that the disappearance of the catalytic activity is due to photosensitiser decomposition, and that the cobalt catalyst was not, in such conditions, the factor limiting H_2 production.

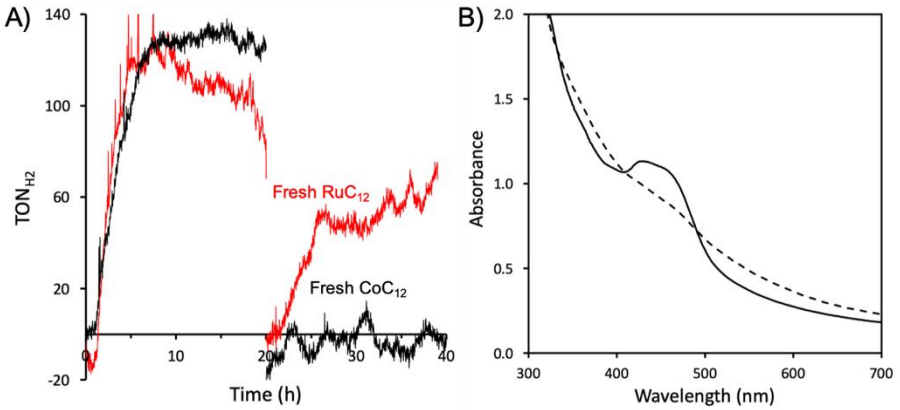

Figure 4.5. (A) Repetitive photocatalytic proton reduction using a liposome mixture consisting of 5 mM DPPC, 50 µM NaDSPE-PEG2K, 50 µM **RuC$_{12}$**, 5 µM **CoC$_{12}$** in argon-saturated 0.1 M NaHAsc and 0.1 M TCEP aqueous solution (3.5 mL, pH = 4.0) at 25 °C. The samples were left in the dark for 1 h and afterwards irradiated with blue light (λ_{irr} = 450 nm, P = 10.6 mW, Φ_0 = 13.7 nmol/s) for 19 h. Afterwards, additional 50 µM **RuC$_{12}$** (red curve) or 5 µM **CoC$_{12}$** (black curve) was added to the reaction mixture and photocatalysis was started again. Bulk concentrations [**RuC$_{12}$**] and [**CoC$_{12}$**] indicate theoretical concentrations assuming no losses during liposome preparation. (B) UV-Vis spectrum of the reaction solution before irradiation (solid line) and after irradiation (dashed line).

Mechanistic considerations. According to Reisner, Hammarström et al,[18] in a 0.1 M $NaHCO_3$ buffer containing 0.1 M NaHAsc the photosensitiser **RuC$_{17}$** (an analogue of **RuC$_{12}$** with 17 carbon atoms per alkyl chain instead of 12) in DMPC:NaDSPE-PEG2K 100:1 liposomes was statically quenched into **RuC$_{17}^{-}$**. The quantum yield of this process was low (0.06), suggesting a low cage escape yield in this system. This effect was attributed to the adsorption of ascorbate to the membrane, which was rendered positively charged by the presence of the cationic metal complex, thereby leading to an overcrowded membrane and slow diffusion of the photogenerated ascorbate radical HAsc$^{\bullet}$. With liposomes containing **RuC$_{12}$** and **CoC$_{12}$**, in absence of TCEP no

reaction took place, so that we assume that in such conditions charge recombination occurred even more quickly. In presence of high concentrations of TCEP, however, the ascorbate radical may be reduced faster by TCEP, thereby allowing **RuC$_{12}^{-}$** to further transfer its electron to the cobalt catalyst and driving H_2 evolution. To test the validity of this hypothesis cyclic voltammetry and differential pulse voltammetry (DPV) analysis was performed for **CoC$_{12}$** (Figure D2). In homogeneous acetonitrile solution, the two first reductions of the hydrogen evolution catalyst were observed at –1.24 V vs Fc/Fc^+ for the $Co^{2+/+}$ couple, and –1.54 V vs Fc/Fc^+ for $Co^{+/0}$. According to these data, the reduced photosensitiser **RuC$_{12}^{-}$** ($Ru^{2+/+}$ = –1.70 V vs Fc/Fc^+ in acetonitrile[17]) is, at least thermodynamically speaking, capable of reducing the catalyst twice, which may trigger hydrogen evolution. On the other hand, the driving force of the second reduction (160 mV) may be insufficient to drive the photocatalytic system at appreciable rates, so that more kinetic studies would be necessary to confirm this mechanism. It should finally be noted that in photocatalytic liposomes oxidative quenching should not be ruled out as it often is in homogeneous conditions, due to the much higher local concentration of the photocatalytic species trapped in the membrane.

In our system, photocatalysis is probably self-inhibited due to the accumulation of $HAsc^-$ at the liposomal surface due to favourable electrostatic interactions with the positively charged **RuC$_{12}$** and **CoC$_{12}$**, which potentially leads to fast charge recombination between the reduced **RuC$_{12}^{-}$** and $HAsc^{\bullet}$.[18] The addition of an excess of TCEP (0.1 M) compared to **RuC$_{12}$** (50 µM), most probably ensures that the reaction between TCEP and $HAsc^{\bullet}$ is faster than the charge recombination process, thus ensuring that **RuC$_{12}^{-}$** can react with **CoC$_{12}$**.

4.3. Conclusion

In conclusion, we demonstrated that **CoC_{12}** is a robust catalyst for photocatalytic proton reduction on liposomes using **RuC_{12}** as photosensitiser. The best photocatalytic activity was observed with a 1:10 ratio of **CoC_{12}** to **RuC_{12}** embedded in DPPC liposomes under fully aqueous conditions with the sacrificial electron donors $HAsc^-$ and TCEP at a pH of 4. In this system, decomposition of the photosensitiser **RuC_{12}** was the factor limiting the photocatalytic production of H_2. Finding a suitable, earth-abundant, alternative to **RuC_{12}** will be required to define the boundaries of **CoC_{12}** as a catalyst for sustainable photocatalytic hydrogen production on liposomes.

4.4 Experimental

4.4.1 General

General methods. ^{1}H NMR and ^{13}C NMR spectra were recorded on a Bruker AV400 MHz spectrometer. Chemical shift values (δ) are reported in ppm relative to the solvent. Electrospray ionisation mass spectrometry (ESI-MS) spectra were measured with a ThermoFischer Scientific MSQ Plus electrospray ionisation mass spectrometer with a 17 – 2000 *m/z* detection range and a resolution of approximately 0.5 *m/z*. TLC-MS was measured on a Plate Express device coupled to an Advion Expression-L Compact Mass Spectrometer with ESI probe (3.5 kV; 250 °C) using as eluent methanol:water:formic acid 90:10:0.1 with a flow of 200 µL min^{-1}. High-resolution mass spectrometry (HRMS) was measured via direct injection on a Thermo Finnagan LTQ Orbitrap with electrospray ionisation. Elemental analysis was performed by Mikroanalytisches Laboratorium Kolbe in Oberhausen, Germany. UV-Vis absorption spectra were measured on a Varian Cary60 spectrophotometer equipped with a single cell Peltier temperature controller at 25 °C using a 3 mL cuvette. Cyclic voltammetry and differential pulse voltammetry were performed using a previously reported set-up.[17]

EPR spectroscopy. CoC_{12} was dissolved in acetonitrile and transferred into a 4 mm outer diameter EPR tube. Continuous wave EPR at X-Band (9.5 GHz) was performed on a Bruker ELEXSYS E680 (Bruker, Rheinstetten, Germany) spectrometer equipped with a TE_{102} cavity and an ESR900 cryostat (Oxford Instrument). Low temperature was achieved with a constant helium flow. The parameters were the following: modulation amplitude 10 G, modulation frequency 100 kHz, power 20 mW, total measurement time 7 min. Simulations were performed on MatLab using Easyspin version 5.2.33.[34]

Materials and reagents. Chemical reagents and solvents were purchased from commercial suppliers and were used without further purification. NaHAsc (≥ 99%) and TCEP were purchased from Merck. The lipids DMPC, DPPC, and DSPC were purchased as dry powders from Avanti Polar Lipids and stored at −20 °C. NaDSPE-PEG2K was purchased as a dry powder from Lipoid and stored at −20 °C. The Avanti Mini-Extruder including polycarbonate extrusion filter (pore size = 0.2 µm, diameter = 19 mm) and filter supports (10 mm) was purchased from Avanti Polar Lipids. di([2,2-bipyridin]6-yl)methanone and **RuC_{12}** were synthesised according to literature.[17,35] $K_3[Fe(C_2O_4)_3]\cdot 3H_2O$ for actinometry was prepared following a literature procedure, kept in the dark, and used within 1 week after preparation.[36]

Preparation of liposomes for photocatalysis. DMPC, DPPC, or DSPC lipids in chloroform (2.0 mL of a 30.6 mM solution), NaDSPE-PEG2K in chloroform (1.0 mL of a 0.613 mM solution), **RuC_{12}** in chloroform (1.0 mL of a 0.613 mM or 0.306 mM solution), and **CoC_{12}** in methanol (1.0 mL of a 0.613 mM, 0.306 mM, 0.0613 mM, or 0.0123 mM solution) were added in a glass pressure-resistant tube. The organic solvents were evaporated under reduced pressure and the resulting lipid film was dried for at least 1 h in *vacuo* to remove residual solvent. The film was then hydrated with a sodium ascorbate (0.1 M) and TCEP (0.1 M) solution (3.5 mL) at pH = 3 – 6, where the pH was adjusted by the addition of 37% HCl to reach pH 3, or by the addition of 1.0 M NaOH to reach pH 4 – 6. Each lipid suspension was subjected to 10 freeze-thaw cycles between liquid N_2 and a 50 °C water bath. Subsequently, the vesicles were extruded 11x with an Avanti Polar Lipids mini-extruder

through a 0.2 µm polycarbonate membrane at 10 °C above the phase transition temperature of the lipid. Assuming no losses during preparation, the resulting liposomes consist of lipid:NaDSPE-PEG2K:**RuC_{12}**:**CoC_{12}**; for example, in the ratio 100:1.0:1.0:0.1 with expected bulk concentrations of 17.5 mM lipid, 0.175 mM NaDSPE-PEG2K, 0.175 mM **RuC_{12}**, and 0.0175 mM **CoC_{12}**. Liposome samples were stored at RT in the dark and used within one week. For photocatalytic H_2 evolution experiments, the liposome solutions were diluted 3.5x with the same aqueous solution as that used for liposome preparation. The size distribution of the hydrodynamic diameter (Z_{ave}) and the polydispersity index (PDI) were measured at 25 °C by dynamic light scattering with a Zetasizer Nano-S from Malvern operating at 632.8 nm with a scattering angle of 173°.

Photocatalytic H_2 evolution. Photocatalytic H_2 evolution was performed using an in-house setup that has been described elsewhere.[29] Here, photocatalytic H_2 production was measured by a Clark hydrogen electrode every five seconds (Unisense H2-NP). The Clark hydrogen electrode was calibrated by a five-time injection of a known amount of high-purity H_2 into the fully deaerated (30 min degassing with argon) thermostated (298 K) photochemical reactor (total volume 25.0 mL) containing milli-Q water (3.5 mL). The calibration was adapted with the pressure change using Logger software, affording direct reading of the volume of H_2 (µL) produced in the gas phase of the reactor. For the photocatalytic H_2 evolution experiments, the thermostated photochemical reactor (25 °C) was charged with the liposome solution (3.5 mL) and a stirring bar and afterwards the system was closed with one rubber septum and two silicon septa. The Clark hydrogen electrode used for measuring the H_2 concentration in the gas phase and two needles (a long one reaching the solution and a short one) were inserted through the septa. The solution was stirred (750 rpm) and degassed by bubbling argon for 30 min. After removal of the needles required for degassing, the data recording was started; first for 1 h (dark measurement), followed by 19 h during light irradiation (light measurement). The irradiation source was an OSRAM Opto Semiconductors LD W5SM LED (λ_{irr} = 450 nm, P = 10.6 mW, Φ_0 = 13.7 nmol/s) equipped with water cooling.

Stability experiments. For the stability experiments, a thin film of either **RuC_{12}** (1.0 mL of a 0.175 mM solution) or **CoC_{12}** (1 mL of a 0.0175 mM solution) was prepared in a glass pressure-resistant tube, using the same methodology as for the preparation of liposomes. The thin film was hydrated with the liposome-containing reaction mixture (3.5 mL) that had been irradiated once for a 19 h photocatalytic H_2 evolution experiment. The liposome solution was then heated for 1 h at 50 °C and every 15 min mixed by vortexing for a few seconds to ensure that most of the thin film of **RuC_{12}** or **CoC_{12}** became solubilised. Afterwards, the solution was transferred back to the photocatalytic set-up and a new H_2 evolution experiment was started, identical to the first one.

Data analysis. The (photocatalytic) turnover number ((P)TON) of the photocatalytic H_2 evolution was calculated from the H_2 production data by 1) converting the produced H_2 in µL to µmol using the molar volume constant (1 mol of ideal gas equals to 22.4 L) and converting µmol to (P)TON by dividing the H_2 production by the catalyst concentration or photosensitiser concentration, respectively; 2) reducing the amount of data of PTON vs time from 14400 data points to 2400 using Origin 9.1 software (data manipulation: reduce by group); 3) data fitting and averaging of three replicate experiments using MATLAB R2020b software to obtain the maximum (P)TON and its standard deviation.

The maximum (photocatalytic) turnover frequency ((P)TOF) of photocatalytic H_2 evolution was obtained using Origin 9.1 software by 1) nonlinear curve fitting of the time evolution of the µmol of H_2 evolved, starting at t = 1 h (category: Growth/Sigmoidal, function: logistic Fit); 2) calculating the first derivative of the H_2 evolution rate = f(t) using mathematics (differentiate) and; 3) averaging three replicate experiments using MATLAB R2020b software to obtain the maximum (P)TOF and its standard deviation.[29]

4.4.2 Syntheses

Synthesis of 1,1-di([2,2'-bipyridin]-6-yl)tridecan-1-ol. A three-neck round-bottom flask was charged with a solution of dodecylmagnesium bromide

(0.50 mL of a 1.0 M solution in diethyl ether, 0.50 mmol) in dry and degassed THF (10 mL). The reaction mixture was cooled to 0 °C and stirred under N_2 atmosphere. A solution of di([2,2-bipyridin]6-yl)methanone (100 mg, 0.296 mmol) in dry and degassed THF (25 mL, RT) was added drop-wise to the cooled Grignard solution. The resulting solution was stirred for 5 h and then quenched with water (50 mL) at RT. The organic layer was extracted with chloroform (3 x 50 mL). The combined organic layers were dried over $MgSO_4$, and the solvents were evaporated under reduced pressure. The crude product was purified via column chromatography (dry-loaded with celite) on silica gel (hexane/acetone = 5:2). The solvents were removed under reduced pressure and the remaining solids were dried *in vacuo*. 1,1-di([2,2'-bipyridin]-6-yl)tridecan-1-ol was obtained as a white solid (yield: 92 mg, 0.18 mmol, 61%). R_f = 0.1 (hexane:acetone 5:2). TLC-MS (ESI) *m/z* found (calcd): 509.1 (509.72, $[M+H]^+$), 531.1, (531.70, $[M+Na]^+$). ^{1}H NMR (400 MHz, $CDCl_3$): δ = 8.67 (dq, *J* = 4.8, 1.3 Hz, 2H), 8.49 (dt, *J* = 8.0, 1.1 Hz, 2H), 8.28 (dd, *J* = 7.7, 1.0 Hz, 2H), 7.93 (dd, *J* = 7.9, 1.0 Hz, 2H), 7.86 (td, *J* = 7.7, 1.8 Hz, 2H), 7.79 (t, *J* = 7.8 Hz, 2H), 7.32 (ddd, *J* = 7.5, 4.8, 1.2 Hz, 2H), 6.69 (s, 1H), 2.49 (m, 2H), 1.54 (m, 2H), 1.22 (m, 48H), 0.87 (t, *J* = 6.8 Hz, 7H). ^{13}C NMR (101 MHz, $CDCl_3$): δ = 163.09 (C_q), 156.09 (C_q), 153.92 (C_q), 149.29 (CH), 137.84 (CH), 137.02 (CH), 123.85 (CH), 121.35 (CH), 121.13 (CH), 119.32 (CH), 78.71 (C_q), 63.13 (CH_2), 42.44 (CH_2), 32.93 (CH_2), 32.04 (CH_2), 32.02 (CH_2), 30.12 (CH_2), 29.82 (CH_2), 29.78 (CH_2), 29.76 (CH_2), 29.74 (CH_2), 29.72 (CH_2), 29.68 (CH_2), 29.56 (CH_2), 29.48 (CH_2), 29.47 (CH_2), 29.45 (CH_2), 25.88 (CH_2), 23.81 (CH_2), 22.81 (CH_2), 22.79 (CH_2), 14.24 (CH_3). LC-MS (ESI) *m/z* found (calcd): 509.4 (509.72, $[M+H]^+$), 531.4 (531.70, $[M+Na]^+$).

Synthesis of CoC_{12}. Cobalt(II) dibromide (13 mg, 0.061 mmol) and 1,1-di([2,2'-bipyridin]-6-yl)tridecan-1-ol (30 mg, 0.059 mmol) were dissolved in methanol (5.0 mL). The reaction mixture was stirred for 4 h under ambient conditions (air, RT). Afterwards, the reaction mixture was concentrated under reduced pressure to 1 mL. Precipitation occurred after addition of diethyl ether (15 mL). The precipitates were collected by filtration and washed with diethyl ether (3 x 5 mL) to obtain **CoC_{12}** as a brown solid (yield: 30 mg, 0.041 mmol, 69%). R_f = 0.3 (hexane:acetone 5:2). ^{1}H NMR (400 MHz, MeOD): δ = 82.13, 67.11, 50.34, 32.37, 18.54, 9.48, 8.74, 8.44, 8.00, 2.30,

1.75, 1.44, 1.26, 1.04, 0.87. LC-MS (ESI) *m/z* found (calcd): 647.8 (647.55, [*M*-Br]$^{+}$). HR-MS (ESI) *m/z* found (calcd): 566.24501 (566.24504, [2*M*-4Br-2H]$^{2+}$), 680.23723 (680.23790, [*M*-2Br+CF_3COO]$^{+}$). Elemental analysis calcd (%) for $C_{33}H_{40}Br_2CoN_4O$: C 54.49, H 5.54, N 7.70; found: C 54.79, H 5.91, N 8.01.

4.5 References

1 T. R. Cook, D. K. Dogutan, S. Y. Reece, Y. Surendranath, T. S. Teets and D. G. Nocera, *Chem. Rev.*, 2010, **110**, 6474–6502.

2 Y. Pellegrin and F. Odobel, *C. R. Chim.*, 2017, **20**, 283–295.

3 A. Pannwitz, D. M. Klein, S. Rodríguez-Jiménez, C. Casadevall, H. Song, E. Reisner, L. Hammarström and S. Bonnet, *Chem. Soc. Rev.*, 2021, **50**, 4833–4855.

4 J. N. Robinson and D. J. Cole-Hamilton, *Chem. Soc. Rev.*, 1991, **20**, 49–94.

5 M. Hansen, S. Troppmann and B. König, *Chem. Eur. J.*, 2016, **22**, 58–72.

6 P. Du and R. Eisenberg, *Energy Environ. Sci.*, 2012, **5**, 6012–6021.

7 M. D. Kärkäs, O. Verho, E. V. Johnston and B. Åkermark, *Chem. Rev.*, 2014, **114**, 11863–12001.

8 J. D. Blakemore, R. H. Crabtree and G. W. Brudvig, *Chem. Rev.*, 2015, **115**, 12974–13005.

9 B. Zhang and L. Sun, *Chem. Soc. Rev.*, 2019, **48**, 2216–2264.

10 M. Hansen, F. Li, L. Sun and B. König, *Chem. Sci.*, 2014, **5**, 2683–2687.

11 B. Limburg, J. Wermink, S. S. van Nielen, R. Kortlever, M. T. M. Koper, E. Bouwman and S. Bonnet, *ACS Catal.*, 2016, **6**, 5968–5977.

12 S. Troppmann and B. König, *Chem. Eur. J.*, 2014, **20**, 14570–14574.

13 S. Troppmann, E. Brandes, H. Motschmann, F. Li, M. Wang, L. Sun and B. König, *Eur. J. Inorg. Chem.*, 2016, **2016**, 554–560.

14 S. Troppmann and B. König, *ChemistrySelect*, 2016, **1**, 1405–1409.

15 R. Becker, T. Bouwens, E. C. F. Schippers, T. van Gelderen, M. Hilbers, S. Woutersen and J. N. H. Reek, *Chem. Eur. J.*, 2019, **25**, 13921–13929.

16 N. Ikuta, S. Y. Takizawa and S. Murata, *Photochem. Photobiol. Sci.*, 2014, **13**, 691–702.

17 D. M. Klein, S. Rodríguez-Jiménez, M. E. Hoefnagel, A. Pannwitz, A. Prabhakaran, M. A. Siegler, T. E. Keyes, E. Reisner, A. M. Brouwer and S. Bonnet, *Chem. Eur. J.*, 2021, **27**, 17203–17212.

18 S. Rodríguez-Jiménez, H. Song, E. Lam, D. Wright, A. Pannwitz, S. A. Bonke, J. J. Baumberg, S. Bonnet, L. Hammarström and E. Reisner, *J. Am. Chem. Soc.*, 2022, **144**, 21, 9399-9412.

19 J. P. Bigi, T. E. Hanna, W. H. Harman, A. Chang and C. J. Chang, *Chem. Commun.*, 2010, **46**, 958–960.

20 M. Guttentag, A. Rodenberg, C. Bachmann, A. Senn, P. Hamm and R. Alberto, *Dalton Trans.*, 2013, **42**, 334–337.
21 R. S. Khnayzer, V. S. Thoi, M. Nippe, A. E. King, J. W. Jurss, K. A. El Roz, J. R. Long, C. J. Chang and F. N. Castellano, *Energy Environ. Sci.*, 2014, **7**, 1477–1488.
22 S. Schnidrig, C. Bachmann, P. Müller, N. Weder, B. Spingler, E. Joliat-Wick, M. Mosberger, J. Windisch, R. Alberto and B. Probst, *ChemSusChem*, 2017, **10**, 4570–4580.
23 N. Queyriaux, E. Giannoudis, C. D. Windle, S. Roy, J. Pécaut, A. G. Coutsolelos, V. Artero and M. Chavarot-Kerlidou, *Sustain. Energy Fuels*, 2018, **2**, 553–557.
24 C. Bachmann, B. Probst, M. Guttentag and R. Alberto, *Chem. Commun.*, 2014, **50**, 6737–6739.
25 C. Bachmann, B. Probst, M. Oberholzer, T. Fox and R. Alberto, *Chem. Sci.*, 2016, **7**, 436–445.
26 D. F. Evans, *J. Chem. Soc.*, 1959, 2003–2005.
27 G. A. Bain and J. F. Berry, *J. Chem. Educ.*, 2008, **85**, 532.
28 P. Müller, B. Probst, B. Spingler, O. Blacque and R. Alberto, *Helv. Chim. Acta*, 2022, **105**, e202100237.
29 C. Liu, D. van den Bos, B. den Hartog, D. van der Meij, A. Ramakrishnan and S. Bonnet, *Angew. Chem. Int. Ed.*, 2021, **60**, 13463–13469.
30 F. Droghetti, F. Lucarini, A. Molinari, A. Ruggi and M. Natali, *Dalton Trans.*, 2022, **51**, 28, 10658–10673.
31 C. Creutz, *Inorg. Chem.*, 1981, **20**, 4449–4452.
32 B. Durham, S. R. Wilson, D. J. Hodgson and T. J. Meyer, *J. Am. Chem. Soc.*, 1980, **102**, 600–607.
33 J. van Houten and R. J. Watts, *Inorg. Chem.*, 1978, **17**, 3381–3385.
34 S. Stoll and A. Schweiger, *J. Magn. Reson.*, 2006, **178**, 42–55.
35 H. Nierengarten, J. Rojo, E. Leize, J.-M. Lehn and A. van Dorsselaer, *Eur. J. Inorg. Chem.*, 2002, **2002**, 573–579.
36 C. G. Hatchard, C. A. Parker and E. J. Bowen, *Proc. R. Soc. Lond. Ser. Math. Phys. Sci.*, 1956, **235**, 518–536.